Interplay of Three-Body Interactions in the EOS of Nuclear Matter

W. Zuo
Institute of Modern Physics, Chinese Academy of Sciences, 730000 Lanzhou, China

A. Lejeune
Institut de Physique, B5 Sart-Tilman, B-4000 Liège 1, Belgium

U. Lombardo
Dipartimento di Fisica, 57 Corso Italia, and INFN-LNS, 44 Via Santa Sofia 95125 Catania, Italy

J. F. Mathiot
Laboratoire de Physique Corpusculaire, Université Blaise-Pascal, CNRS-IN2P3, 24 Avenue des Landais, F-63177 Aubiere Cedex, France

Abstract

The equation of state of symmetric nuclear matter has been investigated within Brueckner approach adopting the charge-dependent Argonne V_{18} two-body force plus a microscopic three-body force based on a meson-exchange model. The effects on the equation of state of the individual processes giving rise to the three-body force are explored up to high baryonic density. It is found that the major role is played by the competition between the strongly repulsive (σ, ω) exchange term with virtual nucleon-antinucleon excitation and the large attractive contribution due to (σ, ω) exchange with $N^*(1440)$ resonance excitation. The net result is a repulsive term which shifts the saturation density corresponding to the only two-body force much closer to the empirical value, while keeping constant the saturation energy per particle. The contribution from (π, ρ) exchange 3BF is shown to be attractive and rather small. The analysis of the separate three-body force contributions allows to make a comparison with the prediction of Dirac-Brueckner approach which is supposed to incorporate via the *dressed* Dirac spinors the same virtual nucleon-antinucleon excitations as in the present three-body force. The numerical results suggest that the three-body force components missing from the Dirac-Brueckner approach are not negligible, especially at high density. The calculation of the nuclear mean field and the effective mass shows that the three-body force affects to a limited extent such properties.

PACS: 25.70.-z; 13.75.Cs; 21.65.+f; 24.10.Cn
Keywords: Nuclear Matter, Brueckner Theory, Three Body Force, EOS

I. INTRODUCTION

It is generally accepted that in order to reproduce the empirical saturation properties of nuclear matter in a non relativistic many-body approach one needs to introduce three-body forces (3BF). Calculations with 3BF have been performed in non-relativistic Brueckner theory [1–4] and in variational approaches [5–7].Moreover in the relativistic Dirac-Brueckner (DB) approach [8–10], 3BF effects are incorporated via the *dressed* Dirac spinors as already stressed by Brown et al. [11].

The existing versions of 3BF applied for nuclear matter calculations are based on either a purely phenomenological model with two parameters adjusted on the empirical saturation point of nuclear matter (and/or the ^3H binding energy) or a microscopic meson-exchange model with nucleonic virtual excitations. In the recent years a general method based on the chiral effective field theory has been developed to systematically generate many-body forces [12].

In the study of nuclear matter the phenomenological TBF has been applied both in variational calculations [5–7] and in Brueckner calculations [4], the microscopic one only in Brueckner calculations [1–3].

The microscopic 3BF is more appropriate to get a deeper understanding of saturation mechanism of nuclear matter and also to extend the study of the equation of state (EOS) to high density. In fact these two aspects of EOS are not necessarily strictly related each other. Moreover it allows to make contact with the DB theory, where the saturation mechanism is interpreted as a purely relativistic effect. It is true in fact that this effect is coming from the $\bar{N}N$ virtual excitations in the scalar σ-meson exchange process due to the *dressed* Dirac spinors in the nuclear medium. But it is just one of the possible contributions to the 3BF and one has to check whether other contributions are important or not.

While the last ten years much studies have been concentrated on the contribution from π and ρ mediated 3BF, in this study we want to emphasize the role played by σ and ω exchange, and in particular the one played by the excitation of the Roper ($N^*(1440)$) resonance in the medium. This is the main motivation of the present study.

The last years the Brueckner many-body approach has done significant progress as concerns the convergence of the hole-line expansion and the validity of the Brueckner-Hartree-Fock approximation. This goal has been reached by means of an accurate estimate of the three-hole line contributions with both the standard and continuous choice for the auxiliary potential [13]. So it seems to be a suitable basis to extend many-body calculations with two-body forces (2BF) to higher order interactions.

The natural framework for 3BF would be the Bethe-Faddeev equation, describing the interaction of three nucleons in nuclear matter. But one may get rid of such a complicate job by a suitable reduction of the 3BF to an effective 2BF, where the correlation effects with the spectator nucleon are correctly provided by the Brueckner iterative procedure.

The purpose of this paper is to revisiting the Brueckner theory of nuclear matter with the 3BF introduced in Ref. [2] performing new calculations where the 2BF is the updated charge-dependent Argonne V_{18}, which reproduces the experimental phase-shifts up to high energy [14]. So we may numerically investigate the role played for the nuclear matter EOS by the different processes giving rise to 3BF and the limitations inherent the relativistic DB approach. Such processes dominate the high density behavior of nuclear matter, which is a

basic input in the studies on the evolution of astrophysical compact objects. Moreover the 3BF effects on the nuclear mean field are also discussed in view of a proper description of the single particle motion in the dynamical simulations of central events of heavy-ion collisions (HIC).

II. MICROSCOPIC THREE-BODY FORCE

The microscopic three-body force adopted in the present calculation is constructed from the meson-exchange current approach as described in Ref. [2]. We refer the reader to this reference for a comprehensive discussion of the model. Let us however recall here its main properties.

In the present understanding of the microscopic structure of nuclei, the NN potential originates from the exchange of mesons. In the OBEP approximation, π, ρ, σ and ω mesons are considered. Once the NN potential is determined, i.e. once the meson-nucleon couplings, form factors and meson masses are fixed, many body forces are uniquely fixed as well. The first candidate to 3BF is the well known Fujita-Miyazawa contribution involving a Δ resonance in the intermediate state with 2π exchange [15]. Extension of this contribution to ρ exchange, together with all other π and ρ exchange contributions have been intensively studied in the past, leading for instance to the Tucson-Melbourne (TM) 3BF [16]. For the present study, we stick to the parametrisation of the TM 3BF, and change only the parameters according to our choice of the NN potential (see below). In terms of meson exchange diagrams, the contributions are shown in Fig. 1a.

More recent studies [12] have been concentrated on the general structure of the 2π 3BF within the framework of chiral perturbation theory. While these studies are important in order to settle the 2π-3BF on first principles according to the symmetry properties of QCD, we do not think they can yet be extended to quantitative investigations of nuclear matter at densities between one to three times normal nuclear matter density. In this domain indeed , the momenta of the exchanged mesons can be large, and the contribution of heavy mesons (σ and ω) are dominating over the 2π-3BF [2]. The 3BF associated to these mesons are shown in Figs. 1b and 1d. They are discussed in more details in Ref. [2]. The $\rho\pi$ and $\rho\sigma$ diagrams, plotted in Fig. 1c, belong to the meson-meson coupling terms which should give a smaller contribution [2] and will not be considered here. More complicated processes could contribute to the 3BF including other nucleonic excitations, but one may expect that the lowest energy excitations, i.e. the isobar $\Delta(1232)$ resonance and the Roper $N^*(1440)$, play the major role in the density domain here considered.

The necessary coupling constants σNN^* and ωNN^* are calculated within the relativistic color dielectric model [17]. The form factors at these vertices are also calculated in this model. Note that because of the orthogonality of the radial wave function of the N and N^*, these form factors cannot have the usual dipole parametrization (as chosen in Ref. [18] for instance). According to Ref. [2] (see Sec. V) they are parametrized as follows:

$$F_{MNN^*}(\vec{k}^2) = \frac{\Lambda^2 + \alpha\vec{k}^2}{\Lambda^2 - \alpha m^2}\left(\frac{\Lambda^2 - m^2}{\Lambda^2 + \vec{k}^2}\right)^2$$

The values of the parameters are reported below (see Table I).

Once the dynamical origin of the NN potential is determined from one boson exchange (OBE) mechanisms, all the parameters needed to determine the 3BF are extracted from the NN potential itself. In the case this NN potential is directly parametrized in terms of OBE potentials, like the Bonn potentials, these parameters are given directly from the fit to NN observables, or NN phase shifts. Instead, in the case it is given in terms of a purely numerical parametrization, like the Paris potential or the AV_{18} potential for instance, one has to extract the equivalent OBE parameters by a direct comparison between various spin-isospin potential in the OBE form and in the parametrized form. This procedure was used in Ref. [2] in order to extract meson exchange parameters from the Paris potential. The π and ρ exchange parameters were determined from the $S = 1$ tensor potential (keeping some of the parameters, like masses and coupling constants, to their physical values), while σ and ω exchange were determined from the central and spin-orbit potentials. In the present calculations, the parameters of the 3BF have been re-determined from the OBE potential model to fulfill the self-consistency with the adopted two-body interaction AV_{18}. It is found that for the σ and ω exchange, the parameters derived from the AV_{18} force remain the same as those given for the Paris potential [2]. While for the π and ρ exchange, the parameters have to be slightly adjusted in order to fit reasonably both the tensor part and the spin-spin part of the AV_{18} potential. The new parameters of the 3BF are collected in Tab. 1. As for the σ-meson mass, the value of 540MeV is still adopted, which has been checked to satisfactorily reproduce the AV_{18} interaction from OBE potential. Varying of the σ-meson mass from $540 MeV$ to $600 MeV$ does not change significantly the self-consistency with AV_{18}, so it is also an interesting point to investigate the effect of the σ-meson mass on the nuclear matter EOS, which is underway and will be presented elsewhere.

Our procedure to determine the parameters of OBE models from a NN potential given in a purely numerical form is of course not unique, nor exact. In particular, the short range part of the potentials is not of the same shape because of the ad-hoc regularization used in the AV_{18} or Paris potentials as compared to the use of form factors in OBE models. These parts of the potential are however of no importance in the contribution of the 3BF to the binding energy of nuclear matter since there are completely washed out by short range correlations (see next section). This procedure assures however that the OBE models used to determine 3BF have a strength and a range for each meson exchange in agreement with the two-body potential.

III. BRUECKNER APPROACH WITH 3BF

The effect of the 3BF is included in the self-consistent Brueckner procedure along the same line as in [1,2], where an effective two-body interaction is constructed without solving the full three-body problem (for a detailed description and justification of the method we refer to Ref. [1,2]). Starting from the 3BF interaction discussed in Sec. II one defines the effective 2BF as

$$< \vec{r}_1\vec{r}_2|V_3|\vec{r}_1'\vec{r}_2' >= \frac{1}{4}Tr\sum_n \int \mathrm{d}\vec{r}_3\mathrm{d}\vec{r}_3'\phi_n^*(\vec{r}_3')(1-\eta(r_{13}'))(1-\eta(r_{23}'))$$

$$\times W_3(\vec{r}_1{}', \vec{r}_2{}'\vec{r}_3{}'|\vec{r}_1\vec{r}_2\vec{r}_3)\phi_n(r_3)(1-\eta(r_{13}))(1-\eta(r_{23})) \qquad (1)$$

where the trace is taken with respect to spin and isospin of the third nucleon. This is nothing else than the average of the three-body force over the wave function of the third particle taking into account via the defect function $\eta(r)$ the correlations between this particle and the two others. The dependence on the defect function entails a selfconsistent determination of the effective 2BF along with the $G-matrix$ and auxiliary potential in that we must re-calculate the effective 2BF at each iterative step and then add it to the bare 2BF for the next loop.

The $\eta(r)$ is actually the defect function averaged over spin and momenta in the Fermi sea and it incorporates, for the sake of simplicity, only the most important partial l-wave components, i.e., the $^1S_0$ and $^3S_1$ partial waves. Corrections due to higher angular momenta in the defect function are expected to be sizeable at high density. They will be included in forthcoming calculations.

The reduction of the 3BF to an effective 2BF is justified by the fact that three-body correlations are small [13], but ultimately one would solve the Bethe-Faddeev equations with 3BF to investigate their effect on the rate of convergence of the Brueckner-Bethe-Goldstone expansion.

IV. NUMERICAL RESULTS

The procedure followed in our calculations is the same as in the usual selfconsistent BHF scheme: The G-matrix is calculated selfconsistently along with the auxiliary potential by solving the Bethe-Goldstone equation [19]. Due to its dependence on the defect function the effective 2BF is calculated selfconsistently at one step of the iterative BHF procedure as said before.

The continuous choice is adopted for the auxiliary potential as it has been already well established that it makes the convergence of the hole-line expansion much faster than the gap choice [13]. It is calculated in a momentum range with cutoff $k_c = 5fm^{-1}$. As bare NN interaction we used the Argonne AV_{18} which gives an excellent fit to NN scattering data as well as to the deuteron binding energy [14]. The partial wave expansion is truncated to $L_{max} = 6$, but the effects of higher partial waves, specially at high density, are to be estimated with further calculations.

A. $\sigma, \omega - \bar{N}N$ 3BF

This subsection is devoted to the discussion of the contribution due to the 2σ exchange diagram with intermediate virtual excitation of a nucleon-antinucleon ($N\bar{N}$) pair (hereafter denoted by $2\sigma - (N\bar{N})$ 3BF). This contribution is worth of particular attention as it is believed to be the main relativistic effect present in DB approach [11,20].

In order to consider separately the effect of the $2\sigma - (N\bar{N})$ 3BF, the calculations have been done by switching off in the self-consistent Brueckner iterative scheme the other 3BF components, i.e., adding only the $2\sigma - (N\bar{N})$ part to AV_{18}. The same procedure has been adopted when calculating the other individual 3BF contributions.

In Fig. 2 the energy shift from the calculation with only bare 2BF due to the $2\sigma - (N\bar{N})$ 3BF is plotted as a function of the nuclear matter density. As expected it gives a repulsive

contribution monotonically increasing with density and approximately fulfills the following power law

$$\Delta E/A \simeq 2.4 \cdot (\rho/\rho_0)^{8/3}(MeV). \tag{2}$$

When the nucleon-nucleon correlations (ladder diagrams) are switched off the repulsion is enhanced since correlations prevent nucleons from getting closer and experiencing a stronger 3BF. The energy shift due to the $2\sigma - (N\bar{N})$ 3BF was also calculated in this approximation (indicated by $\eta = 0$ in the figure) and the results are fit by the same power law but with the prefactor of Eq. (2) enhanced to 3.6 which is close to the value of 4.2 obtained in the crude estimate of Ref. [11].

In the same figure is also reported the relativistic correction to the energy from DB approach, which is defined as the difference between the full DB calculation and its non-relativistic limit, obtained replacing in the DB context the dressed nucleon mass by the bare one [9]. In spite of the different Bonn potentials the shift is almost the same, implying that it is rather insensitive to the two-body interaction adopted. Since the nuclear EOS of DB approach could be quite different from the non relativistic Brueckner approximation, the only meaningful comparison is in fact between the $2\sigma - (N\bar{N})$ contribution and the previous DB correction. Around the saturation density they almost overlap each other and differ at most by 26% at the highest density. This difference is to be attributed to higher order relativistic effects which become only significant at high density. It is clear from the comparison that the most important relativistic correction to the EOS of nuclear matter in DB approach can be reproduced fairly well by BHF calculation including only the 3BF originated from the scalar coupling to the virtual excitation of a nucleon-antinucleon pair. So the accuracy of the DB prediction to the EOS of nuclear matter depends, especially at high density, on to what the extent the other three-body forces cancel each other, and in particular the diagrams involving the excitation of nucleon resonances like the Roper resonance.

In order to push forward the comparison with DB predictions, in Fig. 2 (right side) is also displayed the full energy per particle in different approximations. The $2\sigma - (N\bar{N})$ term provides a noticeable improvement of the saturation density in agreement with the DB results (Bonn B) as compared to the BHF approximation using pure two-body force. The agreement between the two calculations is far beyond what we might expect, the high density deviation being attributed to the defect function reducing the $2\sigma - (N\bar{N})$ 3BF in our calculation. In the same figure is also plotted the result of a complete BHF calculation including all the three-body forces of Fig. 1. Comparing with the BHF EOS it is seen that the full three-body force gives an increasingly strong repulsion to the energy per nucleon in nuclear matter as increasing density. This repulsion is really able to drive the saturation point towards its empirical one. However, looking at the complete Brueckner calculation, i.e. with the full 3BF, one may easily anticipate the importance that processes other than the $2\sigma - (N\bar{N})$ have to shift the saturation energy of about $2MeV$ towards the empirical value.

Besides the scalar σ meson and the nucleon-antinucleon virtual excitations, vector ω meson will also contribute to 3BF. In Fig. 3 are depicted the energy corrections of the different 3BF components from $(\sigma, \omega) - (N\bar{N})$ (left panel) and the corresponding nuclear EOS (right panel). While the $2\omega - (N\bar{N})$ 3BF adds only a comparatively small attractive

contribution, the $\sigma\omega-(N\bar{N})$ component gives a strong repulsion which is even larger than the $2\sigma-(N\bar{N})$ one. Consequently the corresponding EOS turns out to be too stiff and the nuclear matter is underbound at the saturation point with a very low saturation density. So we may conclude that relativistic effects associated to the virtual $N\bar{N}$ excitations cannot reproduce the empirical saturation properties. The 3BF's from nucleon resonances are expected to compensate this too strong repulsion.

B. Effects of 3BF with nucleon resonances and full EOS

In Fig. 4 (left panel) are shown the energy corrections of the 3BF components from nucleon resonances represented in Fig. 1 and the corresponding nuclear EOS's (right panel). The effect of the σ, ω-Roper 3BF turns out to be quite sizeable. As already done in Ref. [2], we include also for consistency the contribution from Roper-Anti-Roper excitations. This contribution is however small, and correct by about 10 % the contribution from the Roper resonance. Their net contribution is attractive and comparable in magnitude to the repulsion from the $\sigma\omega$-$(N\bar{N})$ 3BF as shown in the same figure for comparison.

In Fig. 4 is also reported the π, ρ exchange 3BF, which provides only a relatively small attractive contribution to the energy per nucleon even at high density in agreement with Ref. [2] and it has a little effect on the nuclear EOS.

The competition between all these 3BF's from different sources determines the final EOS of nuclear matter which saturates around $\rho \simeq 0.198\text{fm}^{-3}$ with energy per nucleon $E \simeq -15.08\text{MeV}$ much better than the corresponding value $\rho \simeq 0.265\text{fm}^{-3}$ from the prediction adopting pure AV_{18} two-body force. As compared to the DB approach, the present EOS is much softer at high density. At the corresponding equilibrium density the obtained incompressibility K is about 207 MeV, in agreement with both the empirical value of 210 ± 30 MeV [21]. This nice property should be attributed to the effect coming from the excitation of the Roper resonance, as compared to the strongly repulsive and density-dependent effect coming from $N\bar{N}$ excitations. We recall that this latter effect is the only one present in DB calculations. Despite the BHF EOS exhibits a flatter curvature (see Fig. 2, right side) the compression modulus at the minimum is larger [22] as an effect of the rather large saturation density.

V. SINGLE PARTICLE PROPERTIES

The nuclear mean field is one of the basic inputs in the dynamical simulations of HIC. Transverse flows and other collective observables have been proven to be very sensitive to whether a mean field is taken from a stiff or soft EOS or whether it is given a momentum dependence or not. In central events of HIC high baryonic densities are reached and 3BF effects could become sizeable. This is the main motivation for calculating the mean field and related quantities in our BHF approximation with 3BF.

In the left part of Fig. 5 is shown the 3BF effect on the mean field for two densities $\rho = 0.17$ and $0.34 fm^{-3}$. As expected, the 3BF adds a repulsive contribution to the mean field when increasing the density. The momentum dependence is not much affected because the present 3BF does not introduce any non local effects. This property can be also

seen considering the effective mass derived by the slope of the mean field as a function of momentum. It is defined as

$$\frac{m^*}{m} = \frac{k}{m}\left(\frac{\mathrm{d}e(k)}{\mathrm{d}k}\right)^{-1}, \tag{3}$$

where $e(k)$ is the single particle energy, i.e., $e(k) = k^2/2m + U(k)$ determined self-consistently within the Brueckner approach. The calculated effective mass at the Fermi momentum k_F is depicted in the right part of Fig. 5. It is seen that $m^*(k_F)$ decreases as increasing density for both cases with and without the 3BF. At relatively low density, the 3BF force almost has no effect upon $m^*(k_F)$, while at high density ($\rho \gtrsim 0.2\mathrm{fm}^{-3}$), the 3BF has the effect to saturate $m^*(k_F)$ around a value of 0.72. Therefore the 3BF weakens the depth of the mean field, but does not significantly change the effective mass (around k_F) even at high density (notice the enlarged scale in Fig. 5).

Both calculations with and without the 3BF predict a larger value of $m^*(k_F)$ at high density than the DB approach ($m^*(k_F) = 0.4$ at $\rho = 0.54\mathrm{fm}^{-3}$) and its non-relativistic limit ($m^*(k_F) = 0.449$ at $\rho = 0.54\mathrm{fm}^{-3}$) [9]. This discrepancy might be related to the 'reference spectrum approximation' adopted in the DB approach, which assumes a weak momentum dependence of the relativistic scalar self-energy component and in the non-relativistic limit corresponds to a constant effective mass approximation [9]. It has been shown in Ref. [23] that the above momentum dependence could be strikingly strong for the Bonn potentials.

Another interesting aspect concerning the single particle properties is the *rearrangement* contribution M_2 to the mean field in the hole-line expansion of the mass operator. This term rises from the density functional derivative of the energy per particle in the Brueckner-Hartree-Fock approximation. It brings a sizeable contribution to the Hugenholtz-Van Hove theorem [24], which controls order by order the consistency of the hole-line expansion [25,26]. The 3BF effect on the real part U_2 of the *rearrangement* term M_2, shown in the left side of Fig. 6, is a reduction of at most 6% in the low momentum range. The most sizeable contribution of TBF to the mean field is coming from the functional derivative of three-body energy per particle. The calculation of this contribution requires some additional investigation.

VI. OVERVIEW AND CONCLUSIONS

We have calculated the EOS of symmetric nuclear matter with a microscopic 3BF including the processes depicted in Fig. 1, which are believed to be the most relevant ones. The charge-dependent Argonne V_{18} has been chosen as two-body interaction. The main effect of the microscopic 3BF is to provide that extra-repulsion which, on the one hand, pushes the saturation density towards the empirical value, but, on the other hand, is able to keep a satisfactory value for the saturation binding energy . This is a desirable feature since the empirical saturation energy is already well reproduced by only 2BF, as shown in Fig. 7. In the same figure the results with phenomenological 3BF [4,6,7] are plotted for comparison. The latter gives an EOS comparable with the present one but only in the context of the Brueckner formalism [4]. The prediction from the variational approach exhibits a strong discrepancy with the two others in spite of the rather good agreement at

the level of two-body force (Argonne V_{18}). Otherwise the good agreement with our results show that the phenomenological 3BF works quite well in spite of being so simple (only two adjustable parameters). But its applicability is restricted to only the saturation region, since no constraints can be imposed at higher density.

The effects of the three-body forces from different sources on the nuclear EOS have been investigated and their relative importance has been discussed along with the comparison to the DB approach. It is seen that the $2\sigma - (N\bar{N})$ 3BF alone is able to simulate the most important relativistic correction to the energy per nucleon in the DB approach. The latter can be in fact attributed to a suppression of the attractive σ exchange two-body force felt by a Dirac *dressed* spinor in nuclear medium, which corresponds simply to the $2\sigma - (N\bar{N})$ diagram of Fig. 1d. However the present investigation shows that besides this correction the effects of the 3BF's from other origins could also be very large (for example, those from $\sigma\omega$ exchange and the Roper resonance), and their net contribution is attractive and comparable in magnitude to that of the $2\sigma - (N\bar{N})$ 3BF. As a consequence the repulsion due to the $2\sigma - (N\bar{N})$ 3BF suffers a reduction of about 35% at high density and the EOS turns much softer as compared to both the predictions of the DB [8,9] and relativistic mean field approaches [20].

Finally, the Brueckner-Hartree-Fock mean field and effective mass have been discussed in the present context. The momentum dependence is not so much affected by the 3BF so that the effective mass at the Fermi momentum is quite insensitive to the 3BF up to high density. The effects of 3BF on the rearrangement contribution to the mean field and to the effective mass are quite modest as well.

Acknowledgments:

One of us (W. Z.) would like to thank INFN-LNS and the Physics Department of the Catania University, Italy, for the hospitality extended to him during the time this work was completed.

This work has been supported in part by the Chinese Academy of Science, within the *one Hundred Person Project*, the Major State Basic Research Development Program of China under No. G2000077400.

REFERENCES

[1] A. Lejeune, P. Grangé, M. Martzolff and J. Cugnon, Nucl. Phys. **A453** (1986) 189.
[2] P. Grangé, A. Lejeune, M. Martzolff, and J. -F. Mathiot, Phys. Rev. **C40** (1989) 1040.
[3] A. Lejeune, U. Lombardo and W. Zuo, Phys. Lett. **477** (2000) 45.
[4] M. Baldo, I. Bombaci and G. F. Burgio, Astron. Astrophys. **328** (1997) 274.
[5] R. B. Wiringa, V. Fiks and A. Fabrocini, Phys. Rev. **C38** (1988) 1010.
[6] A. Akmal and V. R. Pandharipande, Phys. Rev. **C56** (1997) 2261.
[7] A. Akmal and V. R. Pandharipande, Phys. Rev. **C58** (1998) 1804.
[8] B. ter Haar and R. Malfliet, Phys. Rev. Lett. **59** (1987) 1652; Phys. Rep. **149** (1987) 207. R. Malfliet, Nucl. Phys. **A488** (1988) 721c.
[9] R. Brockmann and R. Machleidt, Phys. Rev. **C42** (1990) 1965; "The Dirac-Brueckner Approach" in *Nuclear Methods and the Nuclear Equation of State*, Ed. M. Baldo, (World Scientific, Singapore, 1999), Chapt. 2, p. 121.
[10] C. H. Lee, T. T. S. Kuo, G. Q. Li and G. E. Brown, Phys. Rev. **C57** (1998) 3488.
[11] G. E. Brown, W. Weise, G. Baym and J. Speth, Comments Nucl. Phys. **17** (1987) 39.
[12] E. Epelbaum, W. Glöckle, Ulf-G. Meissner, Nucl. Phys. **A671**, (2000) 295.
[13] H. Q. Song, M. Baldo, G. Giansiracusa and U. Lombardo, Phys. Rev. Lett. **81** (1998) 1584.
[14] R.B. Wiringa, V.G. Stoks and R. Schiavilla, Phys. Rev. **C51** (1995) 38.
[15] J. Fujita H. Miyazawa, Prog. Theor. Phys. **17** (1957) 360.
[16] R.G. Ellis, S.A. Coon and B.H.J. McKellar, Nucl. Phys. **A438** (1985) 631.
[17] J.-F. Mathiot, G. Chanfray and H.-J. Pirner, Nucl. Phys. **A500** (1989) 605.
[18] S.A. Coon, M.T. Pena, D.O. Riska, Phys. Rev.**C52** (1995) 2925.
[19] M. Baldo, "The Many-body Theory of the Nuclear Equation of State" in *Nuclear Methods and the Nuclear Equation of State*, Ed. M. Baldo, (World Scientific, Singapore, 1999), Chapt. 1, p. 1.
[20] B. D. Serot and J. D. Walecka, Adv. Nucl. Phys. **16** (1986) 1; Int. Journ. Mod. Phys. **E6** (1997) 515.
[21] J. P. Blaizot, Phys. Rep. **65** (1980) 171.
[22] M. Baldo, M. Bombaci, L. S. Ferreira, G. Giansiracusa and U. Lombardo, Phys. Rev. **C43** (1991) 2605.
[23] L. Sehn, C. Fuchs and Amand Faessler, Phys. Rev. **C56** (1997) 216; T. Gross-Boelting, C. Fuchs, and Amand Faessler, Nucl. Phys. **A648** (1999) 105.
[24] N.M. Hugenholtz and L. Van Hove, Physica **24** (1958) 363.
[25] J. Hüfner and C. Mahaux, Ann. Phys. **73** (1972) 525; J. P. Jeukenne, A. Lejeune and C. Mahaux, Phys. Rep. **25C** (1976) 83.
[26] W. Zuo, I. Bombaci and U. Lombardo, Phys. Rev. **C60** (1999) 024605.

FIGURES

FIG. 1. Diagrams of the microscopic 3BF adopted for the present calculations. This 3BF model is proposed in Ref. [2] based on the meson-exchange approach.

FIG. 2. Left side: $2\sigma - (N\bar{N})$ 3BF contribution to the energy shift from the 2BF energy per particle in symmetric nuclear matter as a function of density. The squares are the results of BHF calculation including nucleon-nucleon correlations and the solid curve denotes simply a fit. The circles are the corresponding BHF results without nucleon-nucleon correlations (i.e., setting $\eta = 0$ in Eq. (1). The dashed curve is a fit. For comparison are also plotted the relativistic corrections in DBHF approach, taken from Ref. [9]. Different symbols distinguish different version of the Bonn potential. Dotted lines are drawn to guide eyes. Right side: EOS of symmetric nuclear matter. The long-dashed curve is the BHF prediction including all 3BF diagrams (Fig. 1). The solid curve corresponds the result using only the 2σ exchange 3BF from the virtual excitation of a $N\bar{N}$ pair. The short-dash one is that using pure AV_{18}. The present results are compared to the DBHF prediction using Bonn B potential (dot-dash curve, from Ref. [9]).

FIG. 3. Left side: Individual (σ, ω)–$(N\bar{N})$ 3BF contributions to the energy shift vs. density Right side: EOS with (σ, ω)–$(N\bar{N})$ 3BF's in comparison to the EOS from both the full 3BF and only pure 2BF

FIG. 4. Left side: Individual contributions to the energy shift due the 3BF from nucleon resonance excitations and from π and ρ exchange. For comparison are also plotted the full 3BF and relativistic energy shifts. The dotted lines are the kinetic energy per particle E_k/A and the two body potential energy per particle E_V/A. Right side: EOS from the left side 3BF components and from pure 2BF in comparison to the full calculation.

FIG. 5. Effects of the 3BF on the mean field vs momentum for a couple of densities (left panel) and the effective mass calculated at $k = k_F$ vs density (right panel). The symbols are the real data, whereas the lines are drawn to guide eyes.

FIG. 6. 3BF effects on the ground state correlations. The *rearrangement* term (real part) in the left side and corresponding effective mass in the right side are plotted vs. momentum for two densities.

FIG. 7. Comparison of the present nuclear EOS with the BHF prediction adopting the phenomenological Urbana 3BF and the variational calculation using the Urbana IX 3BF.

Tab. I - Coupling constants and form factors adopted in the 3BF consistent to the AV_{18} two-body interaction, which are slightly different from that given for the Paris potential (see Ref.[2]). The meson masses are $m_\pi = 138$MeV, $m_\omega = 780$MeV, $m_\rho = 776$MeV, and $m_\sigma = 540$MeV.

	$g^2/4\pi$	Λ (MeV/c)	α
σNN	11.9	1100	
ωNN	33.0	1300	
πNN	14.4	1580	
ρNN	0.55	1300	
σNN^*	2.58	1450	-2.35
ωNN^*	4.13	1550	-2.33

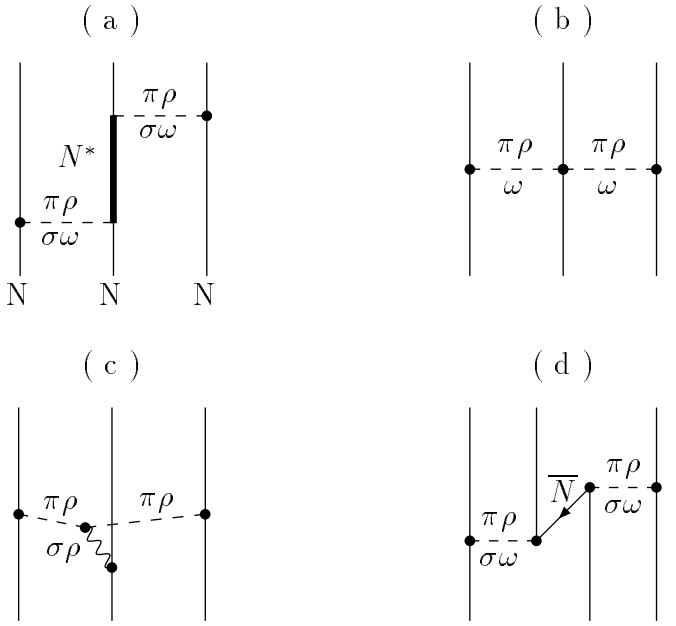
(a)
(b)
(c)
(d)
N^*
$\pi\rho$
$\sigma\omega$
ω
$\sigma\rho$
$\overline{N}$
N
N
N

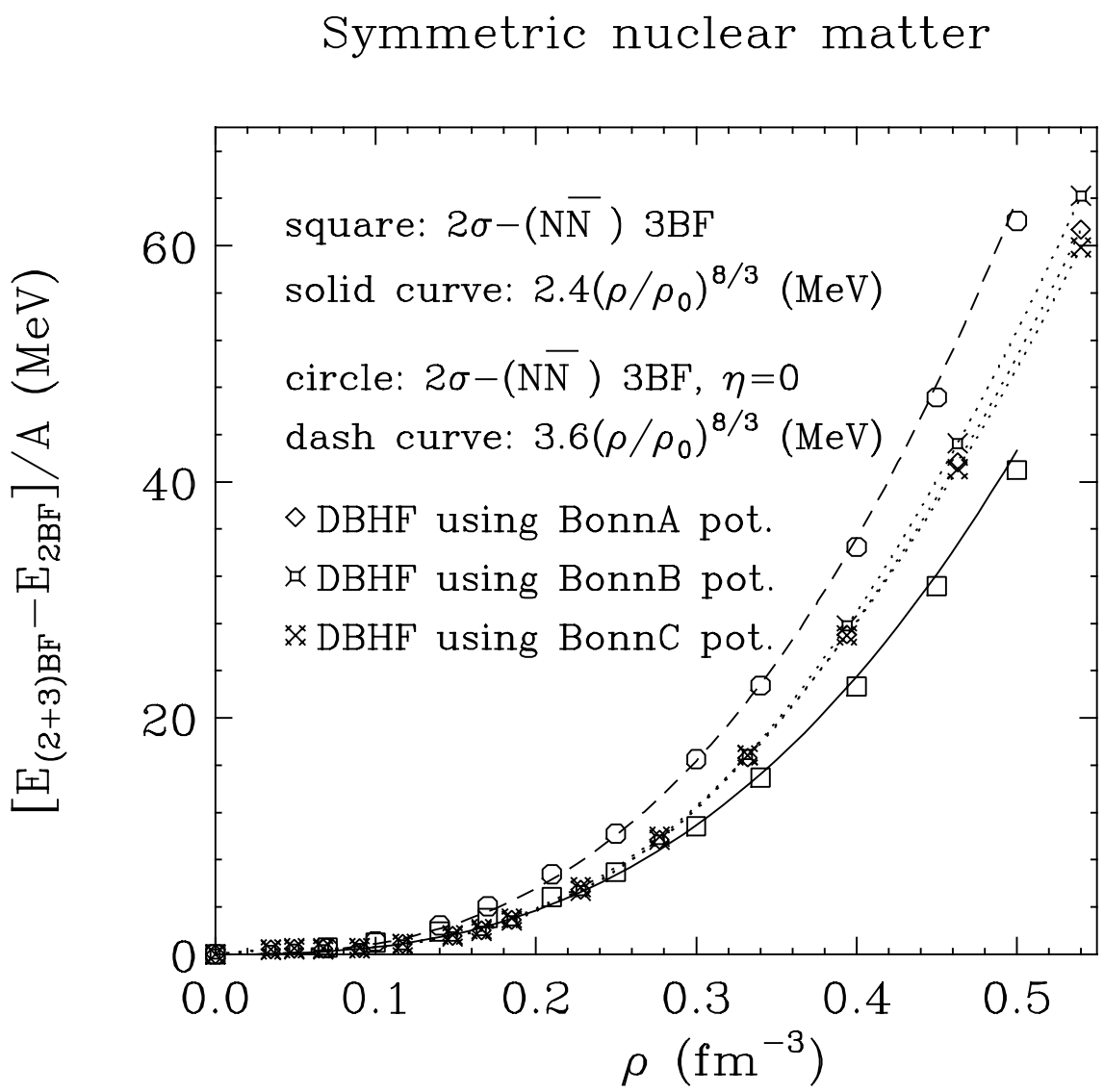
Symmetric nuclear matter
square: 2σ−(NN̄) 3BF
solid curve: 2.4(ρ/ρ0)^8/3 (MeV)
circle: 2σ−(NN̄) 3BF, η=0
dash curve: 3.6(ρ/ρ0)^8/3 (MeV)
◇ DBHF using BonnA pot.
⌑ DBHF using BonnB pot.
⨯ DBHF using BonnC pot.
[E(2+3)BF − E2BF]/A (MeV)
ρ (fm^−3)
0
20
40
60
0.0
0.1
0.2
0.3
0.4
0.5

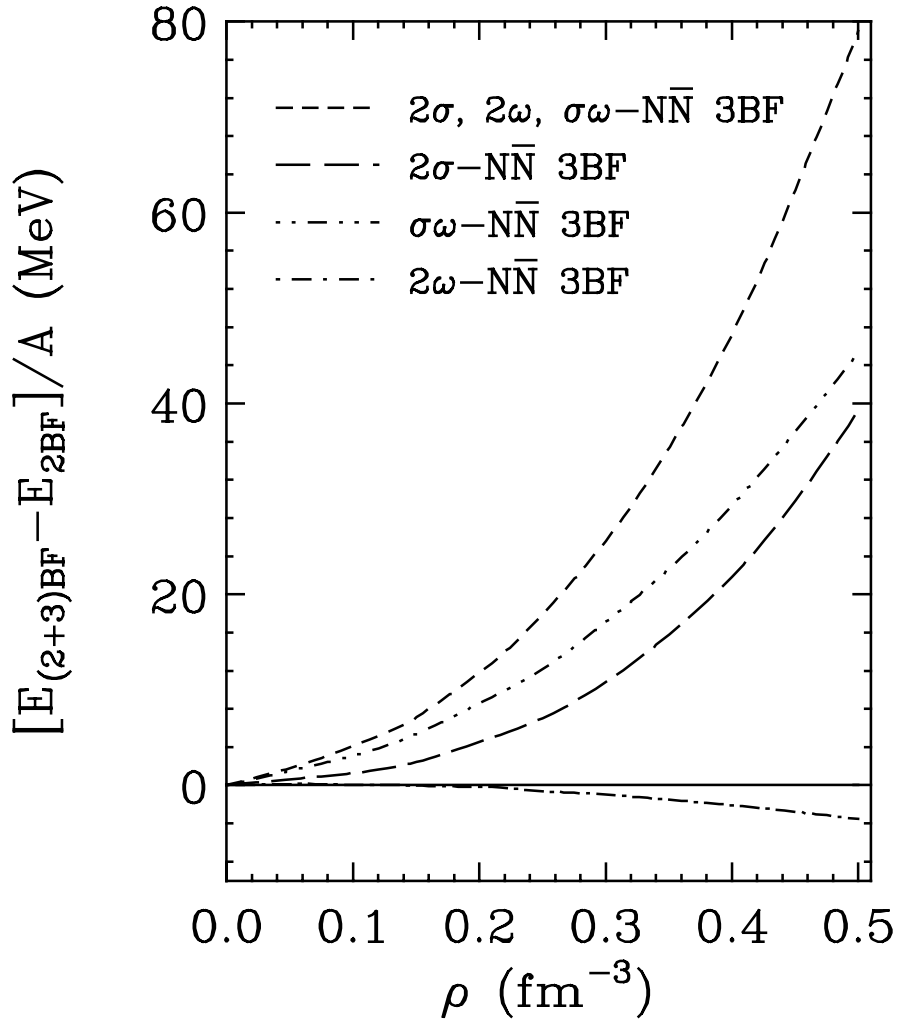
80
60
40
20
0
0.0
0.1
0.2
0.3
0.4
0.5
ρ (fm^{-3})
$[E_{(2+3)BF} - E_{2BF}]/A$ (MeV)
2σ, 2ω, $\sigma\omega-N\bar{N}$ 3BF
$2\sigma-N\bar{N}$ 3BF
$\sigma\omega-N\bar{N}$ 3BF
$2\omega-N\bar{N}$ 3BF

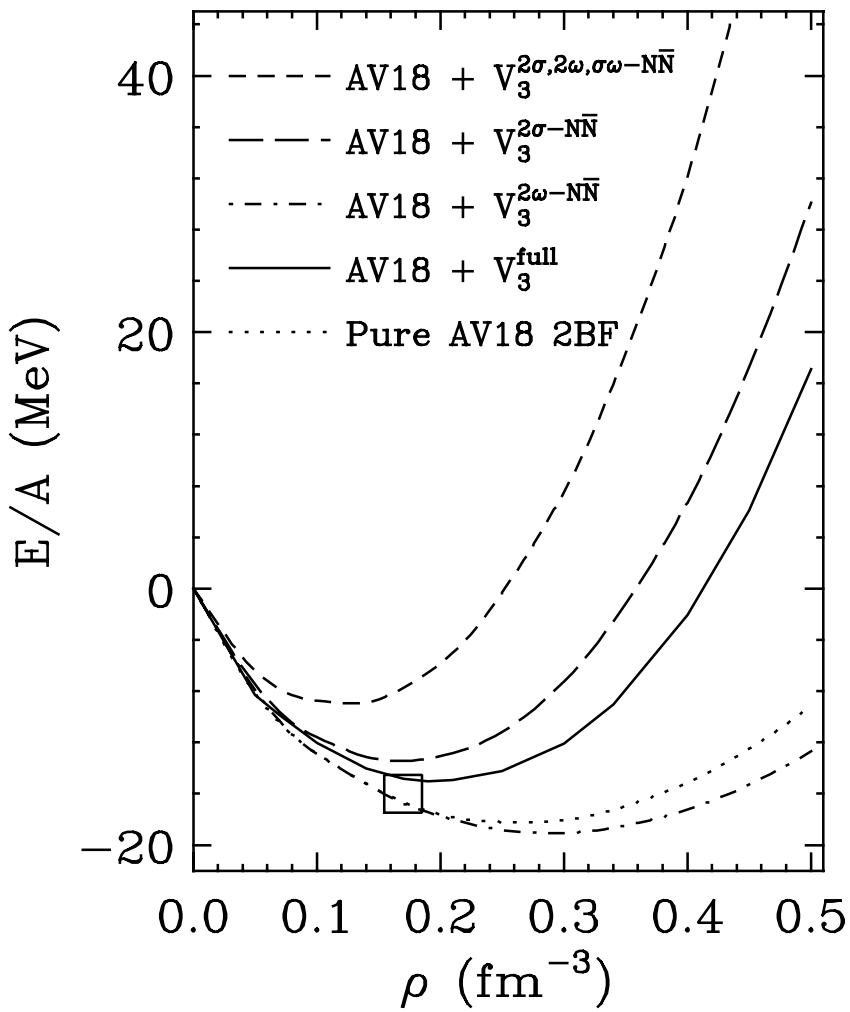
40
20
0
−20
0.0
0.1
0.2
0.3
0.4
0.5
ρ (fm^{-3})
E/A (MeV)
AV18 + $V_3^{2\sigma,2\omega,\sigma\omega-N\bar{N}}$
AV18 + $V_3^{2\sigma-N\bar{N}}$
AV18 + $V_3^{2\omega-N\bar{N}}$
AV18 + V_3^{full}
Pure AV18 2BF

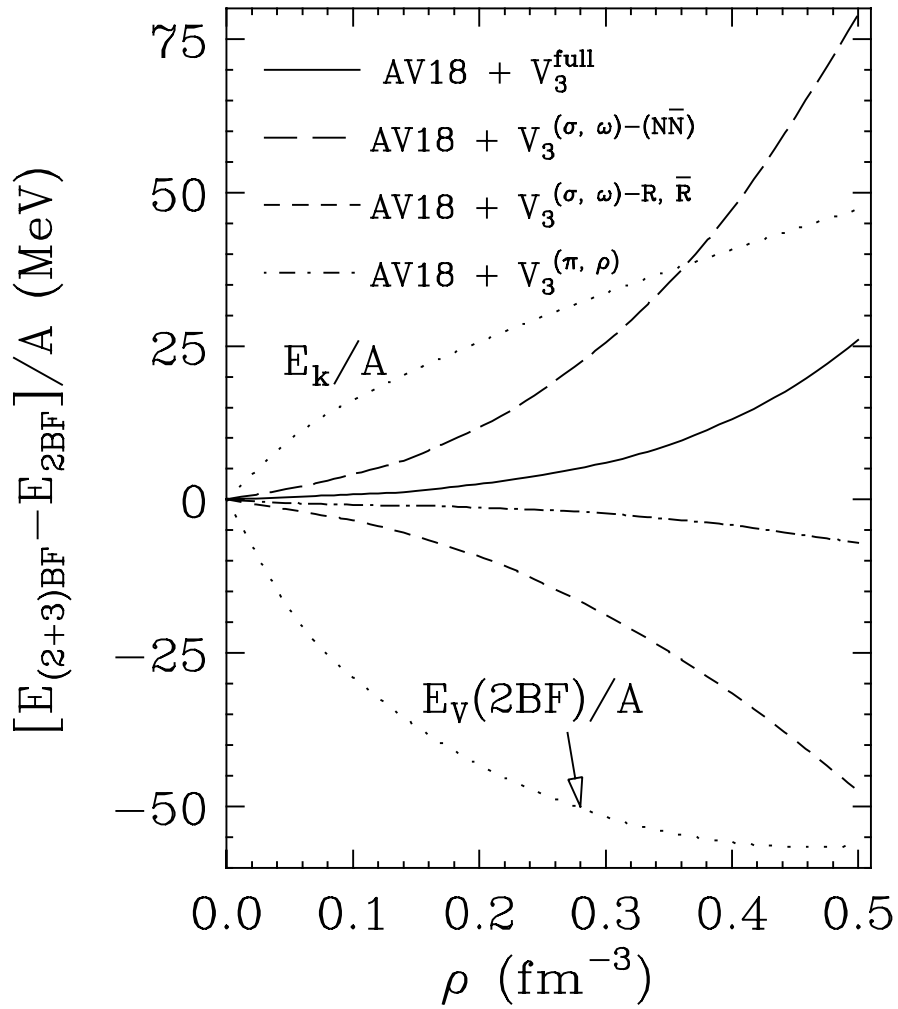
AV18 + V3full
AV18 + V3(σ, ω)−(NN̄)
AV18 + V3(σ, ω)−R, R̄
AV18 + V3(π, ρ)
Ek/A
EV(2BF)/A
[E(2+3)BF − E2BF]/A (MeV)
ρ (fm−3)
75
50
25
0
−25
−50
0.0
0.1
0.2
0.3
0.4
0.5

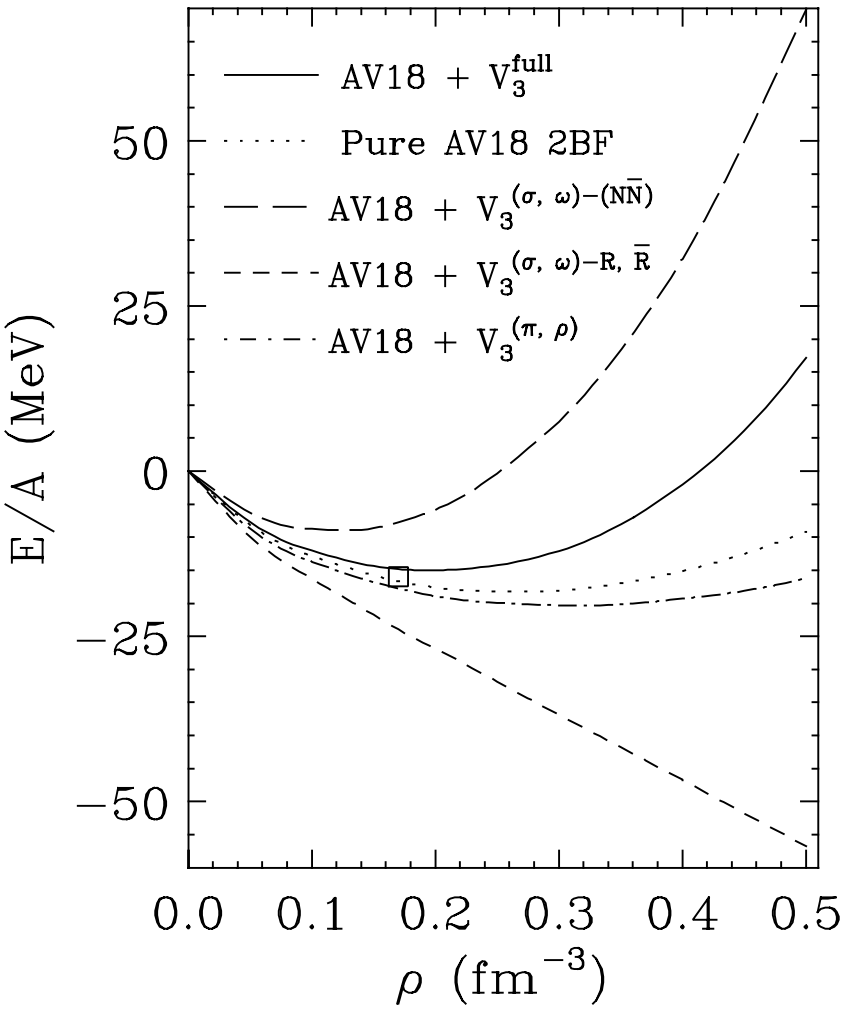
AV18 + V3full
Pure AV18 2BF
AV18 + V3(σ, ω)−(NN̄)
AV18 + V3(σ, ω)−R, R̄
AV18 + V3(π, ρ)
E/A (MeV)
ρ (fm−3)
50
25
0
−25
−50
0.0
0.1
0.2
0.3
0.4
0.5

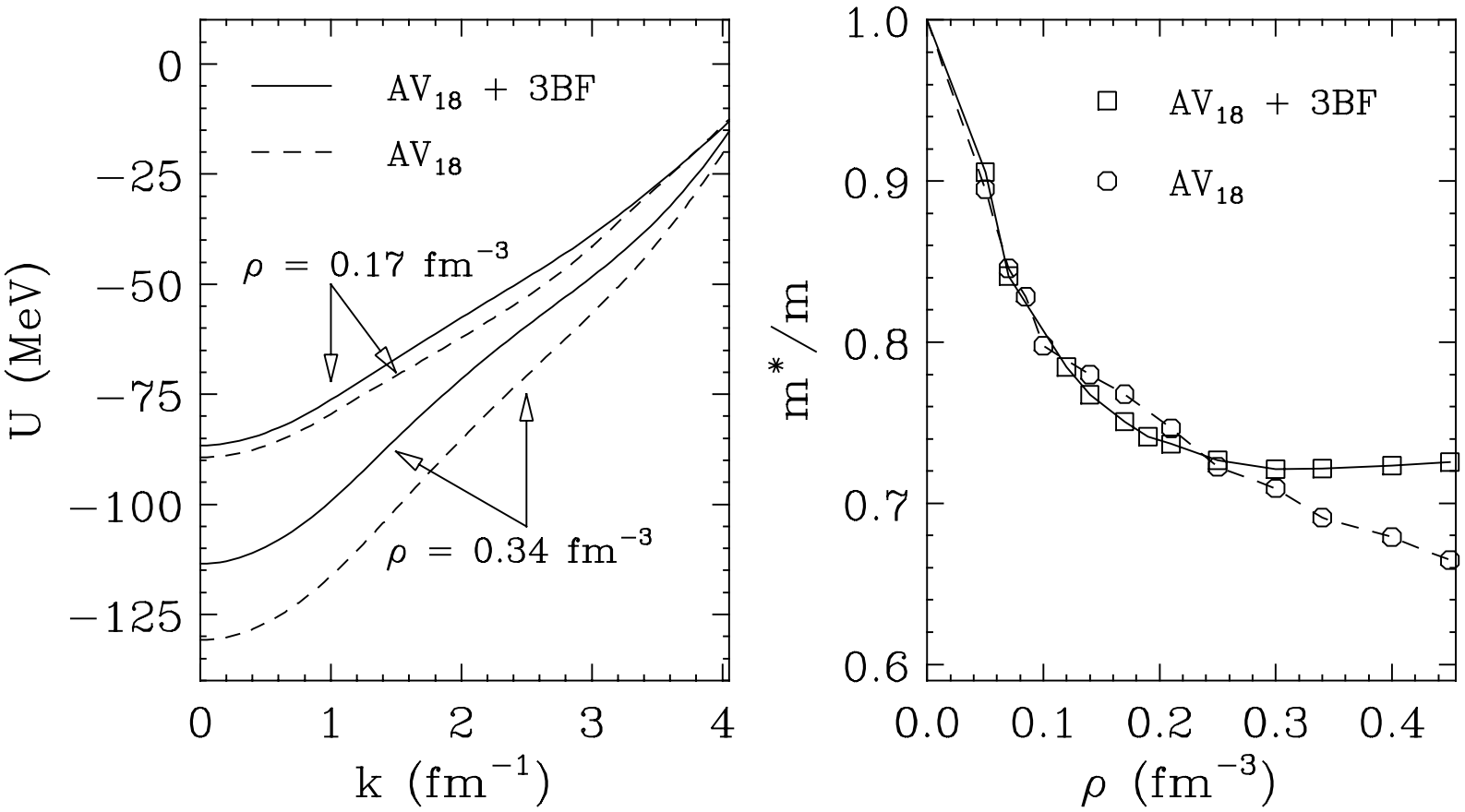
0
−25
−50
−75
−100
−125
U (MeV)
AV18 + 3BF
AV18
ρ = 0.17 fm−3
ρ = 0.34 fm−3
0
1
2
3
4
k (fm−1)
1.0
0.9
0.8
0.7
0.6
m*/m
AV18 + 3BF
AV18
0.0
0.1
0.2
0.3
0.4
ρ (fm−3)

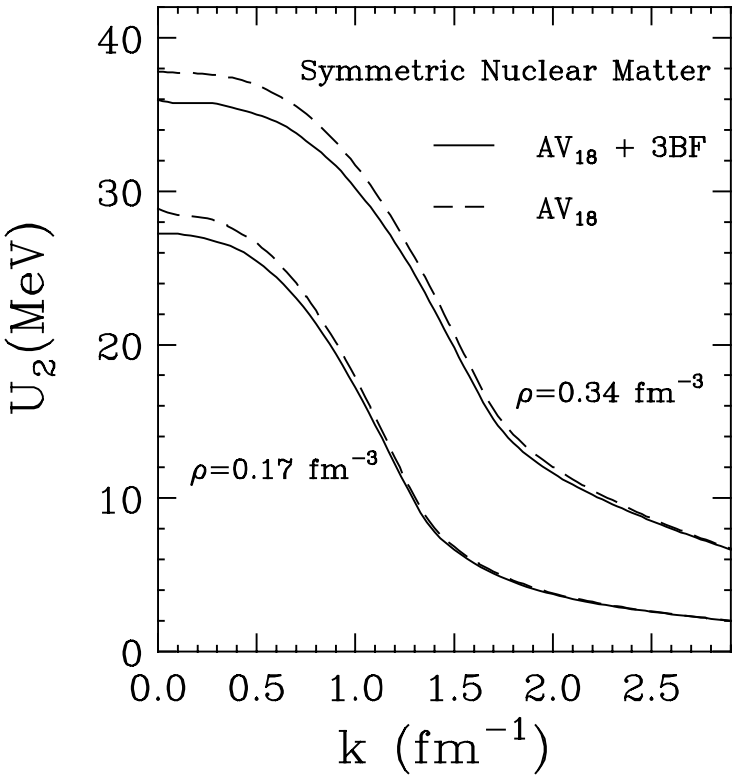
Symmetric Nuclear Matter
AV18 + 3BF
AV18
ρ=0.34 fm−3
ρ=0.17 fm−3
U2(MeV)
k (fm−1)
0
10
20
30
40
0.0
0.5
1.0
1.5
2.0
2.5

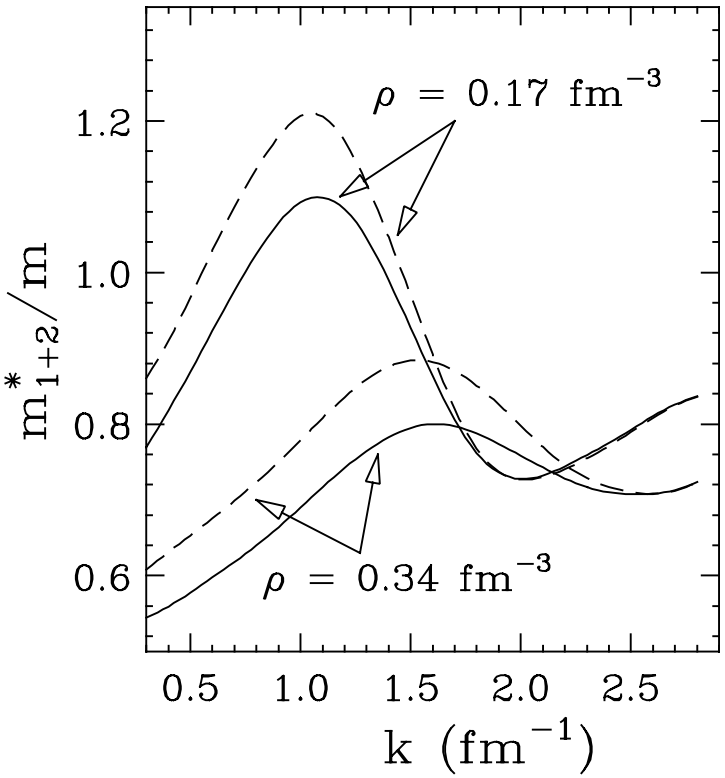
ρ = 0.17 fm−3
ρ = 0.34 fm−3
m*1+2/m
k (fm−1)
0.6
0.8
1.0
1.2
0.5
1.0
1.5
2.0
2.5

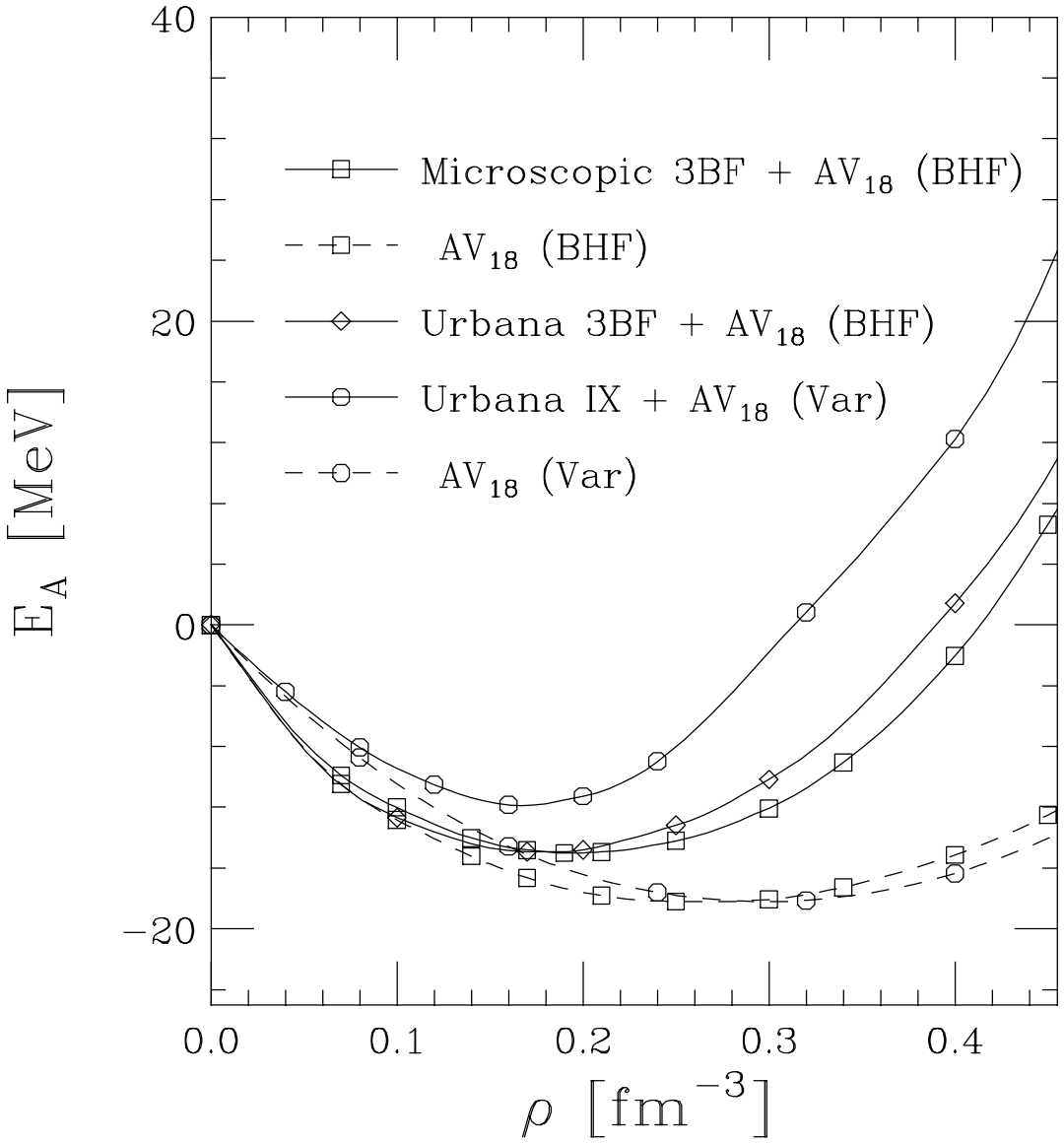
40
20
0
−20
0.0
0.1
0.2
0.3
0.4
E_A [MeV]
ρ [fm^{-3}]
Microscopic 3BF + AV$_{18}$ (BHF)
AV$_{18}$ (BHF)
Urbana 3BF + AV$_{18}$ (BHF)
Urbana IX + AV$_{18}$ (Var)
AV$_{18}$ (Var)